

The 2009 MW 6.1 L'Aquila fault system imaged by 64k earthquake locations

LUISA VALOROSO(*)

INGV, Centro Nazionale Terremoti - Roma, Italy

received 7 February 2016

Summary. — On April 6 2009, a MW 6.1 normal-faulting earthquake struck the axial area of the Abruzzo region in central Italy. We investigate the complex architecture and mechanics of the activated fault system by using 64k high-resolution foreshock and aftershock locations. The fault system is composed by two major SW dipping segments forming an en-echelon NW trending system about 50 km long: the high-angle L'Aquila fault and the listric Campotosto fault, located in the first 10 km depth. From the beginning of 2009, foreshocks activated the deepest portion of the mainshock fault. A week before the MW 6.1 event, the largest (MW 4.0) foreshock triggered seismicity migration along a minor off-fault segment. Seismicity jumped back to the main plane a few hours before the mainshock. High-precision locations allowed us to peer into the fault zone showing complex geological structures from the metre to the kilometre scale, analogous to those observed by field studies and seismic profiles. Also, we were able to investigate important aspects of earthquakes nucleation and propagation through the upper crust in carbonate-bearing rocks such as: the role of fluids in normal-faulting earthquakes; how crustal faults terminate at depths; the key role of fault zone structure in the earthquake rupture evolution processes.

1. – Introduction

A key feature to investigate earthquake mechanics is the detailed description and characterisation of fault zone structure and kinematics. In the last 15 years, by improving the available seismological datasets and earthquake location techniques, we have upgraded the resolution capability of the available earthquake location catalogues by more than one order of magnitude.

In Italy, we progressed from the reconstruction of the geometry of the main fault segments at the kilometre scale during the 1997 MW 6.0 Colfiorito seismic sequence

(*) E-mail: luisa.valoroso@ingv.it

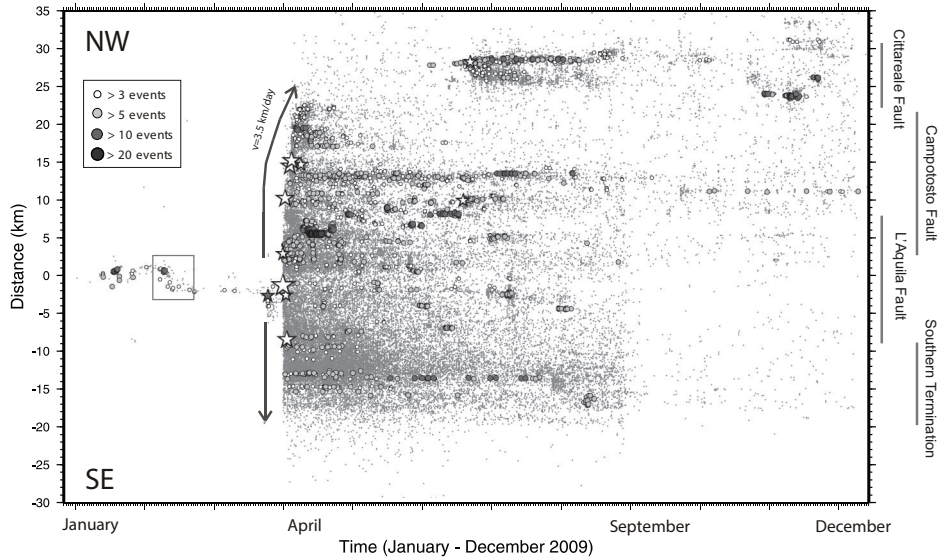


Fig. 1. – Spatiotemporal evolution of the seismicity in the epicentral area during the whole 2009. White stars are events with MW larger than 5 plus the MW 4.0 foreshock (30 March), the MW 4.4 (22 June), and the MW 3.9 occurred in the Cittareale area (25 June). The y -axis represents a 65 km long N133-trending vertical plane (intersecting the L’Aquila main shock) where we project all the events of the sequence. Gray arrows indicate the directions of seismicity migration (see text for explanation). We also report the location of 425 clusters of similar earthquakes. Events are color-coded according to the number (N) of events in each cluster. Modified after Valoroso *et al.*, (2013).

(*e.g.*, [1]), to the identification and description of secondary structures tens of metres long for the 2009 MW 6.1 L’Aquila fault, retrieving a fault anatomy that finally resembles the degree of complexity observed by field geologists on fault outcrops (*e.g.*, [2]).

For the L’Aquila sequence, high-quality seismological data were recorded by a dense network of seismic stations installed over the epicentral area made up of 67 3-component continuously recording seismic stations. The network included 20 permanent stations of the Italian Seismic National Network (RSNC) located within 80 km from the epicentral area, while 47 temporary stations were installed soon after the occurrence of the mainshock to record the aftershock sequence, through the coordination of rapid-response seismic networks from Italy, France and Germany [3]. The deployment of such a dense emergency network during the seismic crises improved the detection capacity of the local and regional networks, through lowering the detectable magnitude threshold.

These improvements in seismic data acquisition have been associated in the last years to efforts made to develop automatic procedures that allow reliable detection and accurate location of seismic events in large earthquake catalogues (*e.g.*, [4, 5]; and references therein).

By taking advantage of these recent major improvements in data acquisition, archiving and analysis, we have been able to build up the largest earthquake catalogue ever recorded for a moderate-magnitude normal-faulting event, composed of 64,000 high-precision aftershock locations covering the whole 2009 (fig. 1). The dataset has been processed by means of an accurate automatic picking procedure (*e.g.*, [4]) together

with cross-correlation analysis and relocated with the double-difference relative location methods ([5] and references therein) reaching a completeness magnitude for the catalogue equal to 0.7 (all the details on the processing of the dataset are reported in [6]). The combined use of these procedures results in earthquake location uncertainties in the range of a few metres to tens of metres (*i.e.*, lower than the spatial dimension of the source of the earthquakes).

Here, we summarize the major characteristics of the spatiotemporal seismicity distribution of the foreshock-aftershock sequence and we report on the fine-scale three-dimensional fault zone internal structure and kinematics of the activated fault system. Also, we report on the presence of clusters of similar earthquakes in order to give insights on the mechanical properties of the activated fault segments.

2. – The seismic sequence

The MW 6.1 L'Aquila mainshock occurred on the 6th of April 2009 at 01:32 UTC, following a long-lasting sequence of foreshocks starting around 4 months before and culminating with a MW 4.0 foreshock on March 30 (grey star in fig. 1, in which we show the space-time distribution of the 64k earthquakes through all of 2009). The mainshock hypocentre was situated directly below the town of L'Aquila (fig. 2), causing 308 deaths and significant damage to buildings in the area.

Despite the moderate magnitude of the main event, the 2009 seismic sequence is an extraordinary case study thanks to the availability of a very high-quality seismological, geodetic and geomorphological datasets. Results for this best worldwide-instrumented normal-faulting earthquake, revealed a strong earthquake rupture complexity of the main event in terms of: rupture directivity and slip velocity ([7] and reference therein). Additional information on fault zone properties and crustal heterogeneity affecting the mainshock rupture evolution were derived from seismic tomography studies [8]. Soon after the mainshock, evidence for 13 km of surface ruptures, partially interpreted as a direct expression of coseismic fault rupture, was observed by field geologists (thick grey lines in fig. 2; [9]). Moreover, post-seismic deformation was measured on and adjacent to the observed surface ruptures by 3D terrestrial laser scan (TLS) technology and GPS ([10,11]).

2.1. Spatiotemporal seismicity evolution: evidences of fluids involvement in the mainshock nucleation process and aftershock sequence migration. – The MW 6.1 mainshock was preceded by a foreshock sequence that lasted at least for 4 months (fig. 1). The spatiotemporal evolution of the foreshock sequence shows many interesting aspects. During the first 3 months of 2009, foreshocks clustered at the deepest portion of the main L'Aquila fault plane within the nucleation volume along an about 10 km long NW-trending segment (grey dots in map in fig. 2); the week before the mainshock, the largest foreshock (MW 4.0) occurring on March 30 (dark grey star in figs. 1 and 2) activated a minor antithetic off-fault segment with seismicity migrating rapidly toward the surface; finally, a few hours before the mainshock, the seismicity jumped back to the main fault that ruptured during the 2009 April 6 MW 6.1 main event [12].

Interestingly, a peculiar migration of seismicity along the base of the L'Aquila fault toward the nucleation zone of the MW 4.0 foreshock and the MW 6.1 main event has been observed from 10 to 20 February 2009 (square inset in fig. 1). This migration of foreshocks, which occurred at a speed of 0.5 km/day towards a fault patch characterized by a low b-value of 0.7 [13], coincides with a transient signal in the GPS time series,

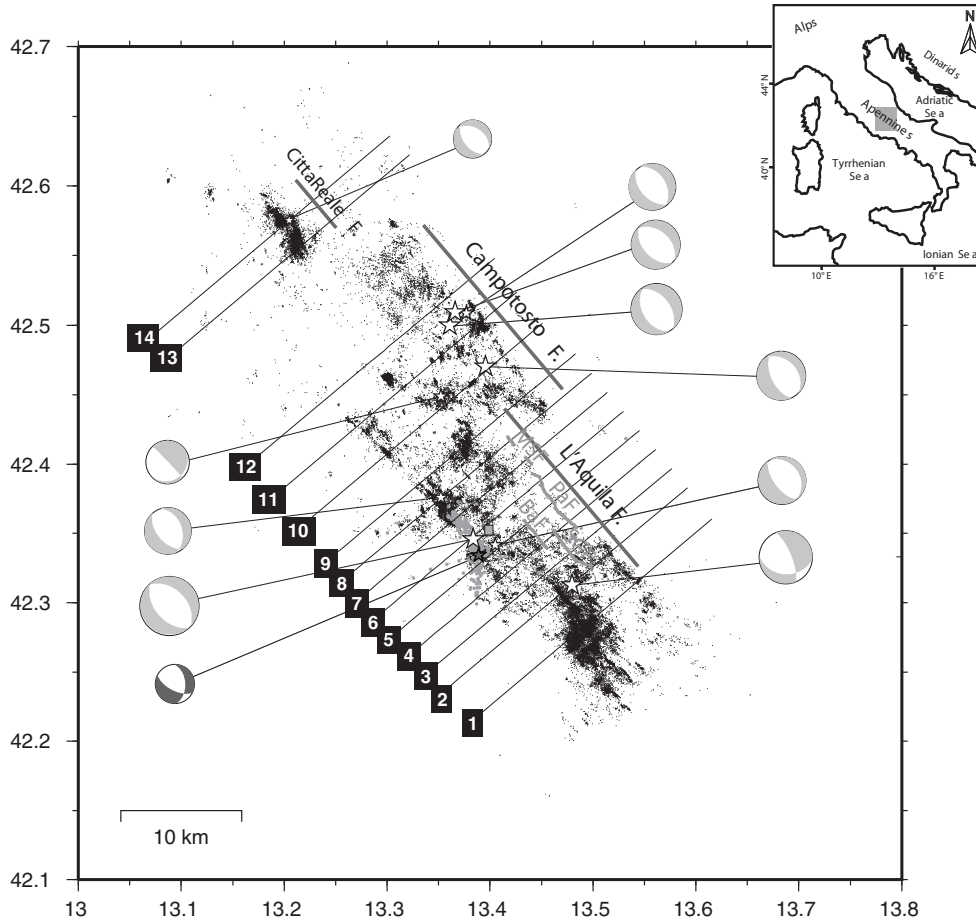


Fig. 2. – Map view of the foreshock and aftershock sequence (grey and black dots, respectively) of the 2009 L'Aquila earthquake. Stars represent the location of the largest events of the sequence. Black lines indicate the vertical sections reported in fig. 3, showing earthquakes occurring within 2 km from the vertical plane. We also report the focal mechanism of the largest events (from [14]). Dark gray lines are a schematic representation of the three main-fault segments activated during the sequence, while light grey lines represent the coseismic surface ruptures from [9] along the Monte Stabiate (MSF), Paganica-San Demetrio (PaF), Bazzano (BaF) and San Gregorio (SGF) geological faults.

that has been interpreted as a precursory transient slow-slip event loading the MW 6.1 seismic volume [15]. The presence of clusters of similar earthquakes at the base of the L'Aquila segment, occurring in the same time window (see white and grey dots in the same inset in fig. 1) furnishes further support to the idea of a stress loading at the base of the L'Aquila fault during the foreshock sequence.

After 20 February 2009, seismicity kept occurring within the nucleation volume until the occurrence of the MW 4.0 foreshock (grey star in fig. 1). After the large MW 4.0 foreshock, seismicity migrated off-fault (fig. 1) and changes in other geophysical parameters were observed. In particular, the MW 4.0 event marked the beginning of an

abrupt temporal change in the VP/VS ratio and crustal anisotropy [16], the b -value [13], the elastic parameters of the crustal volume surrounding the earthquake source [17], the frequency content of fault zone trapped waves [18].

The observed variations of elastic and anisotropic parameters of the seismic-wave propagation properties together with the spatiotemporal foreshock sequence evolution are the signature of a complex sequence of dilatancy and fluid diffusion processes affecting the rock volume surrounding the nucleation area. It is worth noting that a similar behaviour has been observed during other normal-faulting earthquakes occurred along the Apennines within carbonate-bearing rocks. One example is represented by the 1997 Umbria-Marche earthquake characterized by a foreshock sequence and a prolonged series of moderate events rupturing multiple fault segments (*e.g.*, [19-21]).

On April 5, seismicity jumped back to the L'Aquila plane with a MW 3.9 foreshock, followed by the MW 6.1 main event a few hours later [12].

Soon after the mainshock, aftershocks activated the southeasternmost sector (grey arrow pointing to SE in fig. 1), where the unilateral rupture of the main shock was observed [7]. Then, seismicity migrated toward NW, with a migration rate on the order of 3.5 km/day [12] (curved line pointing upward in fig. 1), where three MW 5 events activated the Campotosto fault. A pore pressure diffusion process has been invoked to model the observed seismicity migration toward the north-western sector [12, 22], suggesting that the activation of adjacent segments is promoted by fluid pressure diffusion processes advancing along the fault system.

At the end of June, a minor seismicity cluster developed near the Cittareale village, following a MW 3.9 event (figs. 1 and 2). The seismicity pattern of the Cittareale cluster, with events progressively migrating outward from the MW 3.9 event, suggests the involvement of a pore pressure relaxation process. Similar cases of seismicity migration following moderate (*i.e.*, MW 4) magnitude events have been observed along the Apennines. Examples are the MW 3.8 2010 Pietralunga sequence ([23, 24]) and the MW 3.9 2013 Gubbio sequence [25, 26], which occurred on a sector of the Northern Apennines where a series of deep boreholes testified the presence of fluid (CO₂) overpressure at shallow depth.

By the end of 2009, the maximum length of the fault system imaged by the earthquake distribution was about 50 km in the N135E-trending direction.

3. – Geometry, kinematics and mechanics of the L'Aquila fault system

To show the fault architecture we plot aftershock epicenters in map view and we construct a set of 14 vertical sections oriented N50E, perpendicular to the general strike of the major fault segments, where we project events located within ± 1 km from each vertical plane (fig. 3). In each vertical section, we report the location of the mapped co-seismic surface ruptures reported by [9] along the Monte Stabiata (MSF) and Paganica-San Demetrio (PaF) fault (thick grey lines in fig. 2). Also, we show the regional moment tensor solutions computed by [14] for the 11 events with MW larger than 4.4 (grey beach balls). The only exceptions in terms of moment magnitude are for the MW 4.0 foreshock and for the MW 3.9 Cittareale event.

The fault system is composed by two main SW dipping segments, the L'Aquila and the Campotosto faults, forming a 50 km long en-echelon system trending in the NW direction. The L'Aquila fault breaks the entire upper crust from 10 km depth to the surface, dipping 50 degrees (± 2) to the SW, showing a length of about 18 km in the N135E direction (sections 3 to 8 in fig. 2). The fault architecture is complicated by

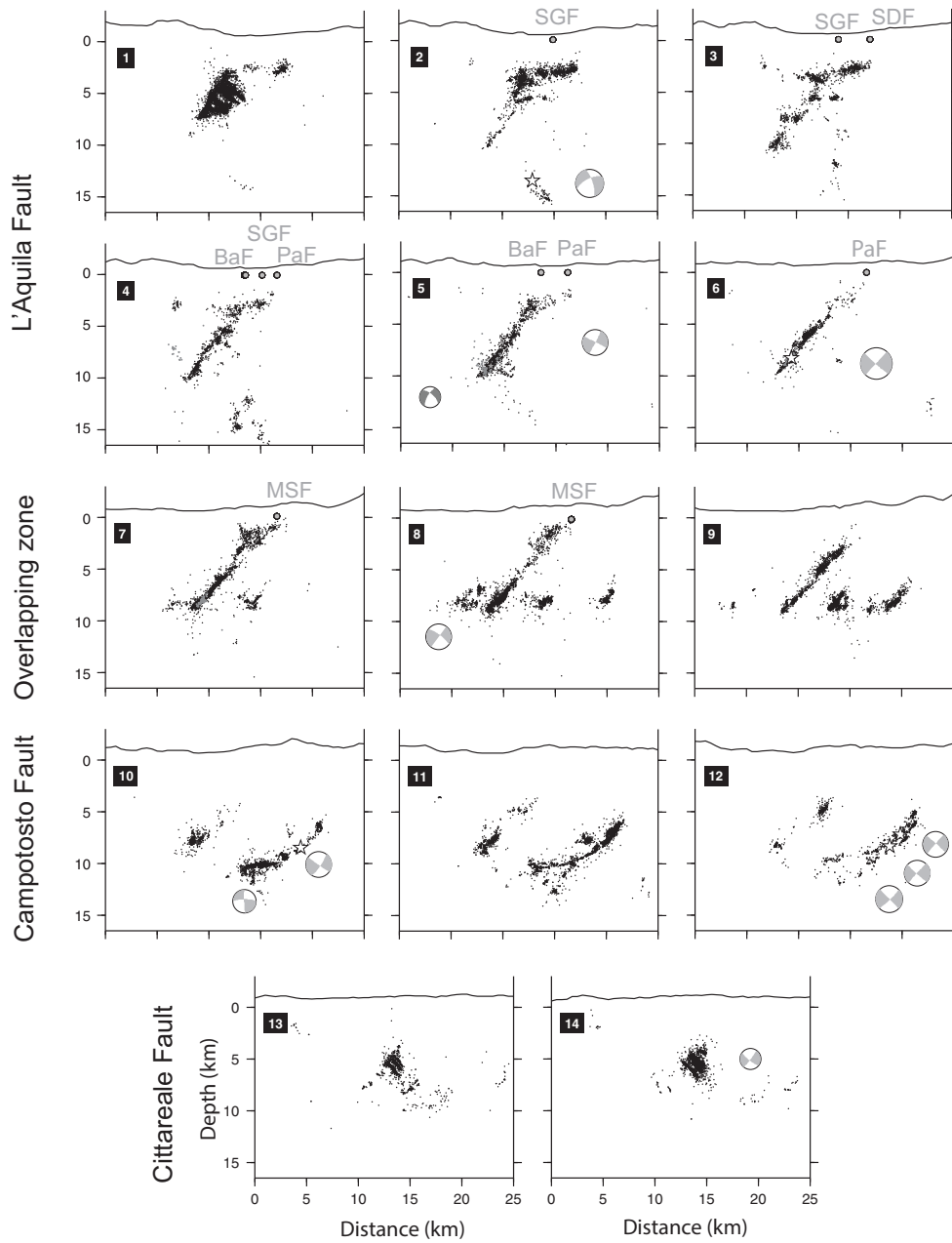


Fig. 3. – Set of 14 vertical sections showing the foreshocks (grey dots), aftershocks (black dots) and large events (white stars) distribution at depth, along with their focal mechanisms. The location of the intersections between the vertical sections and the coseismic surface rupture faults reported in fig. 2, is also reported (grey dots). We indicate the major fault segments activated during the sequence. From SE toward NE: the L'Aquila segment, the overlapping zone, the Campotosto segment and the Cittareale cluster.

a complex pattern of small (tens of metres) secondary faults associated with the main fault.

Traversing along strike from SE to NW (*i.e.*, from section 2 to 9 in fig. 3), we observe that aftershocks are aligned along a thin plane, few tens of metres wide, between 10 and 3 km of depth (section 2). In section 3, aftershocks are distributed to define a thicker plane (500 m thick), showing minor synthetic and antithetic subsidiary structures, tens of metres long, occurring both in the L'Aquila fault hanging-wall and footwall. In the seismic volume where the mainshock occurs (section 6), the fault plane is continuous between 10 to 3 km of depth, showing an irregular distribution of aftershocks on the rupture plane along dip: the plane is thin at the base where the mainshock nucleates and thickens going upward. The retrieved fault image resembles the complex geometry of a dilational jog or bend observed by field geologists on outcrops of normal faults (*e.g.*, [2]). At shallower depths, multiple thin antithetic and synthetic splays branch off the main fault plane (section 7 in fig. 3).

Most of the focal mechanism solutions of events nucleating on the L'Aquila fault have pure dip-slip kinematics with one of the two nodal planes dipping at high angle to SW, consistent with the aftershock alignment. We find a geometrical correspondence between the coseismic ruptures mapped at the surface along the Monte Stabiata (MSF), the Paganica-San Demetrio (PaF) and the San Gregorio (SGF) geological faults (grey traces in fig. 2 and grey dots in the vertical sections in fig. 3) and the surface projection of the seismically imaged L'Aquila fault. The L'Aquila fault terminates to the SE, in correspondence to an abrupt increase in geometrical complexity; here, the seismicity is distributed among a dense network of minor thin structures and does no longer occur on a principal fault plane (sections 1 and 2 in fig. 3).

The Campotosto fault, activated by three events with MW in the 5.0 to 5.2 range, shows a striking listric geometry, composed by planar segments with different dips along depth rather than a smoothly curving single-fault surface (see sections 10 to 12 in fig. 3). A minor Cittareale fault was activated by the end of June 2009 at the northern termination of the fault system (fig. 1 and sections 13–14 in fig. 3).

The image of this en-echelon fault system composed by two-kilometre scale major faults, is complicated by secondary structures, tens to hundreds of metres long, such as: fault splays toward the surface (section 7); bends and cross-fault intersections along the main-fault width; numerous syn- and antithetic fault segments located both in the hanging- and foot-wall of the two major faults (see sections 7 to 9).

A remarkable feature in the geometry of the entire fault system is the abrupt seismicity cut-off around 9 km of depth (fig. 3). In the Campotosto segment, the cut-off coincides with a nearly horizontal active basal discontinuity imaging a listric geometry. Below the L'Aquila fault segment this feature is less outstanding, but seismic activity does image a sub-horizontal discontinuity at the base of the high-angle fault (sections 6 to 8 in fig. 3). The spatiotemporal distribution of clusters of similar events can help to shed light on the mechanical behaviour of this basal discontinuity. A large number of clusters of similar events nucleate at the seismicity cut-off depths [6], at the juncture between high-angle SW-dipping normal faults and the low-angle flat discontinuity. In fig. 4, where we show the distribution of the 2009 seismicity along with clusters of similar earthquakes (white and light grey dots) along a down-dip section of the L'Aquila fault, we can appreciate that the largest number of clusters are all located at the base of the seismogenic fault. Then, we speculate in favour of the presence of a major rheological transition around 10 km of depth where the stress concentrates between high-angle normal brittle faults that undergo unstable sliding and a basal velocity-strengthening (*i.e.*, creeping) discontinuity.

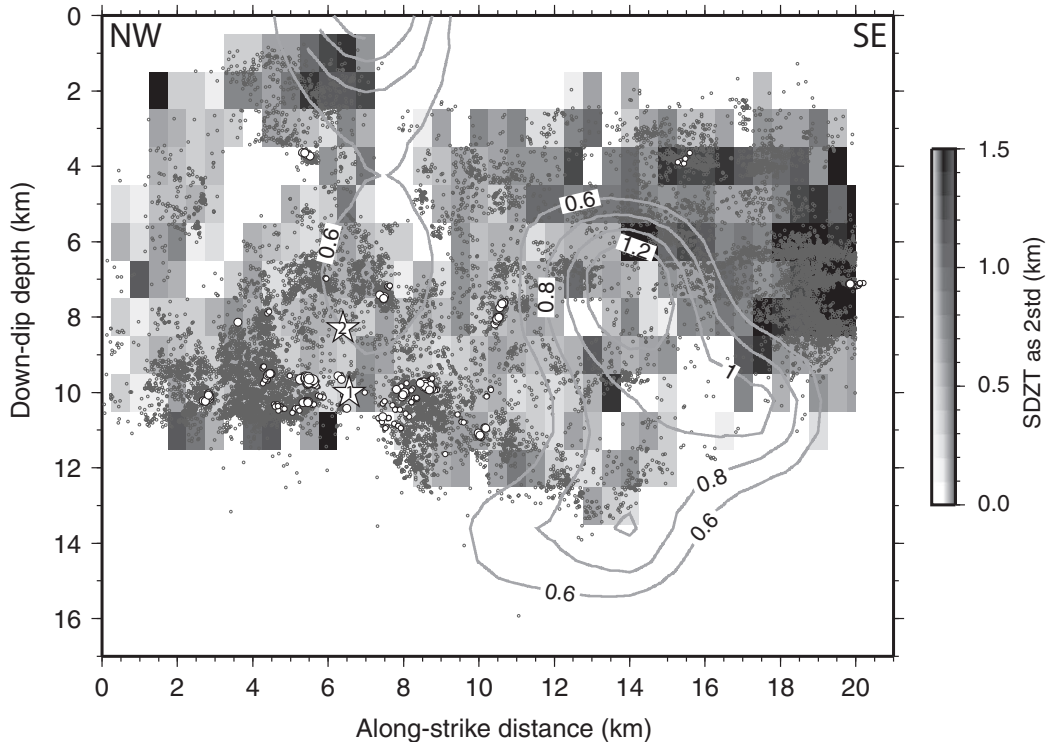


Fig. 4. – Downdip fault section along the L’Aquila fault plane (modeled by Cirella *et al.* in [7]) showing events occurring within 3 km from the fault plane (grey dots), the emergent and impulsive mainshock hypocenters (white stars from [8]), the location of clusters of similar earthquakes (white dots) and the coseismic slip distribution (gray solid contours) computed by Cirella *et al.* in [2]. Seismological damage zone thickness (SDZT) after Valoroso *et al.* (2014).

This interpretation may support the observation of a precursory slow-slip event loading stress on the L’Aquila fault at seismogenic depths where the MW 4.0 foreshock and the MW 6.1 mainshock nucleated [15]. We also speculate that this feature, characterizing this portion of the Central Apennines, might generally describe how crustal normal faults terminate at depth in carbonate bearing rocks.

4. – L’Aquila fault zone structure: the key role of fault zone properties in the earthquake rupture evolution processes

Taking advantage of the large dataset of high-precision aftershock locations, we reconstructed the internal structure of the L’Aquila normal fault by investigating the thickness of the fault damage zone (fig. 4). The fault zone is composed by a thin zone of localized deformation where the largest events nucleate (white stars), bordered by a zone of intense fracturing characterized by variable widths along strike and depth defining what we have called a seismological damage zone (SDZ). The SDZ is narrow in the central portion of the fault (0.3 km) where the rupture nucleated and propagated updip at very high speed (4 km/s; [7]) and within the main coseismic slip patches; whereas it becomes thicker where the rupture propagated along strike toward the SE, with a lower rupture

velocity (2.53 km/s; [7]). The rupture propagation stopped where the geometry of the fault becomes complex and the SDZ shows its maximum width (1.5 km in fig. 4; see also the geometry of the fault in vertical section 1 in fig. 3). The remarkable correspondence between the complex geometry and the place where the rupture speed decelerates gives insights on how geometrical complexities of the fault plane interact and sometimes counteracts with the co-seismic rupture evolution.

A last interesting data we report on the L'Aquila earthquake regards the complex rupture onset of the MW 6.1 event and how it has been affected by the fault zone velocity structure [8]. The initial stage of the mainshock rupture is characterized by an emergent phase (EP, star 1 in fig. 4) followed by an impulsive phase 0.87 s later (IP, star 2 in fig. 4). The local velocity structure computed by using seismic tomography [8] indicates that the EP onset is located in a very high P -wave velocity and relatively low Poisson-ratio region; whereas the IP hypocentre is located just outside the low Poisson-ratio region and marks the beginning of the large moment release ([7]; see the contours of the coseismic slip distribution reported in fig. 4). Then, the comparison between the spatial variations of P -wave and Poisson-ratio velocity structure within the mainshock nucleation volume with the rupture history indicates that heterogeneity of lithology and material properties along the L'Aquila fault played an important role during the rupture nucleation and propagation, despite the moderate magnitude of the L'Aquila event.

* * *

Results summarized in this work originate from a wealth of scientific papers published over the years about this complex and extremely well-monitored moderate-magnitude event. I wish to thank my colleagues Lauro Chiaraluca, Cristiano Collettini, Raffaele Di Stefano, Davide Piccinini, David P. Schaff and Felix Waldhauser for the huge help in the high-precision seismic catalogue compilation and for constructive discussions about the L'Aquila seismic sequence. I also thank those at INGV dealing with seismological data collection and archiving for making available and maintaining very good-quality data and Daniele Melini for maintaining the INGV HPC-computer facilities. Finally, I thank Luigi Improta and Antonio Meloni for the invitation to the 2015 SIF conference.

REFERENCES

- [1] CHIARALUCE L., ELLSWORTH W. L., CHIARABBA C. and COCCO M., *J. Geophys. Res.*, **108 B6** (2003) 2294 doi:10.1029/2002JB002166.
- [2] VALOROSO L., CHIARALUCE L. and COLLETTINI C., *Geology*, **42** (2014) 343.
- [3] MARGHERITI L. *et al.*, *Ann. Geophys.*, **54** (2011) 392 doi:10.4401/ag-4953.
- [4] ALDERSONS F., DI STEFANO R., CHIARALUCE L., PICCININI D. and VALOROSO L., *Eos Trans. Am. Geophys. Union*, **90** (2009).
- [5] WALDHAUSER F. and SCHAFF D., *J. Geophys. Res.*, **113** (2008) B08311 doi:10.1029/2007JB005479.
- [6] VALOROSO L., CHIARALUCE L., PICCININI D., DI STEFANO R., SCHAFF D. and WALDHAUSER F., *J. Geophys. Res.*, **118** (2013) 1156 doi:10.1002/jgrb.50130.
- [7] CIRELLA A., PIATANESI A., TINTI E., CHINI M. and COCCO M., *Geophys. J. Int.*, **190** (2012) 607 doi:10.1111/j.1365-246X.2012.05505.x.
- [8] DI STEFANO R., CHIARABBA C., CHIARALUCE L., COCCO M., DE GORI P., PICCININI D. and VALOROSO L., *Geophys. Res. Lett.*, **38** (2011) L10310 doi:10.1029/2011GL047365.
- [9] BONCIO P., PIZZI A., BROZZETTI F., POMPOSO G., LAVECCHIA G., DI NACCIO D. and FERRARINI F., *Geophys. Res. Lett.*, **37** (2010) L06308 doi:10.1029/2010GL042807.

- [10] CHELONI D. *et al.*, *Geophys. J. Int.*, **181** (2010) 1539 doi:10.1111/j.1365-246X.2010.04584.x.
- [11] SERPELLONI E., ANDERLINI L. and BELARDINELLI E., *Geophys. J. Int.*, **188** (2012) 473 doi:10.1111/j.1365-246X.2011.05279.x.
- [12] CHIARALUCE L., VALOROSO L., PICCININI D., DI STEFANO R. and DE GORI P., *J. Geophys. Res.*, **116** (2011) B12311 doi:10.1029/2011JB008352.
- [13] SUGAN M., KATO A., MIYAKE H., NAKAGAWA S., VUAN A., *Geophys. Res. Lett.*, **41** (2014) 6137 doi:10.1002/2014GL061199.
- [14] SCOGNAMIGLIO L., TINTI E., MICHELINI A., DREGER D. S., CIRELLA A., COCCO M., MAZZA S. and PIATANESI A., *Seismol. Res. Lett.*, **81** (2010) 892 doi:10.1785/gssrl.81.6.892.
- [15] BORGHI A., AOUDIA A., JAVED F. and BARZAGHI R., *Geophys. J. Int.*, **192** (2016) 776 doi:10.1093/gji/ggw046.
- [16] LUCENTE F. P., DE GORI P., MARGHERITI L., PICCININI D., DI BONA M., CHIARABBA C. and AGOSTINETTI N. P., *Geol.*, **38** (2010) 1015 doi:10.1130/G31463.1.
- [17] ZACCARELLI L., SHAPIRO N. M., FAENZA L., SOLDATI G. and MICHELINI A., *Geophys. Res. Lett.*, **38** (2011) L24304 doi:10.1029/2011GL049750.
- [18] CALDERONI G., ROVELLI A. and DI GIOVAMBATTISTA R., *Geophys. Res. Lett.*, **42** (2015) 1750 doi:10.1002/2015GL063176.
- [19] RIPEPE M., PICCININI D. and CHIARALUCE L., *J. Seismol.*, **4** (2001) 387.
- [20] MILLER S. A., COLLETTINI C., CHIARALUCE L., COCCO M., BARCHI M. R. and BORIS J. P. K., *Nature*, **427** (2004) 724 doi:10.1038/nature02251.
- [21] ANTONIOLI A., PICCININI D., CHIARALUCE L. and COCCO M., *Geophys. Res. Lett.*, **32** (2005) L10311 doi:10.1029/2004GL022256.
- [22] MALAGNINI L., LUCENTE F. P., DE GORI P., AKINCI A. and MUNAFÒ I., *J. Geophys. Res.*, **117** (2012) B05302 doi:10.1029/2011JB008911.
- [23] MARZORATI S., MASSA M., CATTANEO M., MONACHESI G. and FRAPICCINI M., *Tectonophysics*, **610** (2014) 91 doi:10.1016/j.tecto.2013.10.014.
- [24] CHIARALUCE L., *J. Struct. Geol.*, **42** (2012) 2 doi:10.1016/j.jsg.2012.06.007.
- [25] DE GORI P., LUCENTE F. P. and CHIARABBA C., *J. Geophys. Res.*, **42** (2014) 2157 doi:10.1002/2015GL063297.
- [26] CHIARALUCE L. *et al.*, *Ann. Geophys.*, **57** (2014) S0327 doi:10.4401/ag-6426.